0026-895X/97/020262-07$3.00/0

MOLECULAR PHARMACOLOGY, **51**:262–268 (1997).

1,5-Benzothiazepine Binding Domain Is Located on the Extracellular Side of the Cardiac L-Type Ca^{2+} Channel

JUNKO KUROKAWA, SATOMI ADACHI-AKAHANE, and TAKU NAGAO

Department of Toxicology and Pharmacology, Faculty of Pharmaceutical Sciences, University of Tokyo, 7–3-1 Hongo, Bunkyo-ku, Tokyo 113, Japan

Received July 22, 1996; Accepted October 19, 1996

SUMMARY

To determine whether 1,5-benzothiazepine Ca^{2+} channel blocker approaches its binding domain within the cardiac L-type Ca^{2+} channel from inside or outside of the membrane, we tested the effects of a novel potent 1,5-benzothiazepine derivative (DTZ323) and its quaternary ammonium derivative (DTZ417) on guinea pig ventricular myocytes by using the whole-cell patch-clamp technique. The extracellular application of DTZ417 suppressed the L-type Ca^{2+} channel currents ($I_{Ca(L)}$) with an IC_{50} value of 1.2 ± 0.02 μM, which was close to the IC_{50} value of diltiazem (0.63 ± 0.01 μM). The suppression of $I_{Ca(L)}$ by DTZ417 was voltage and use dependent but lacked tonic block, which allowed us to investigate the onset of the effect on $I_{Ca(L)}$ by changing the holding potential (HP) from −90 to −50 mV in the presence of DTZ417. DTZ417 did not have significant effects on $I_{Ca(L)}$ at an HP of −90 mV. At −50 mV, DTZ417 (50 μM) applied from the extracellular side completely suppressed $I_{Ca(L)}$, whereas it had no effect from the intracellular side. DTZ323 (1 μM) also inhibited $I_{Ca(L)}$ only from the extracellular side, without any effects by the intracellular application of ≤10 μM. However, a quaternary phenylalkylamine derivative, D890 (0.1 mM), acted only from the intracellular side. These results suggest that in contrast to the phenylalkylamine binding site, in cardiac myocytes the 1,5-benzothiazepine binding site is accessible from the extracellular side of the L-type Ca^{2+} channel.

Three major types of Ca^{2+} channel blockers (i.e., DHPs, PAAs, and BTZs) bind to distinct, high affinity binding sites on the α_1 subunit of the L-type Ca^{2+} channel (1–4).

The binding domains for DHP and PAA have been localized using photoaffinity labeling and immunoprecipitation as well as expressed chimeric channels (5–10). However, photoaffinity labeling does not label the exact binding site that is critical for the pharmacological effect, and chimeric channels may alter tertiary structure. Thus, electrophysiological studies have been required for determination of the validity of the binding sites predicted by photoaffinity labeling and chimeric channel experiments.

Through electrophysiological techniques, permanently charged derivatives of DHP and PAA, which are considered to be impermeable through the cell membrane, have been used to determine the sidedness of these binding domains. These electrophysiological data have indicated that the binding domain for PAA is located on the intracellular side of the membrane in cardiac (11) and skeletal (12) myocytes, whereas the DHP binding site is accessible from the extracellular side (13).

However, the binding site for BTZ has not been identified because of a lack of high affinity ligands for the BTZ site. Results of recent photoaffinity labeling and immunoprecipitation studies have suggested that the binding site for diltiazem-like Ca^{2+} channel blockers is located in the linker region between segments S5 and S6 of domain IV (14, 15).

A novel potent Ca^{2+} channel blocker, DTZ323 {(+)-*cis*-3-(acetyloxy)-5-[2-[[2-(3,4-dimethoxyphenyl)ethyl]-methylamino]ethyl]2,3-dihydro-2-(4-methyoxyphenyl)-1,5-benzothiazepine-4(5*H*)-one} (Fig. 1), has been recently introduced as the most potent BTZ derivative (16). In rabbit crude T tubule membranes, DTZ323 exhibited complete inhibition of [^{3}H]diltiazem binding (16). K_i values indicated that DTZ323 (K_i = 6.6 nM) was 48 times more potent than diltiazem. The specific binding of [^{3}H]DTZ323 to the membranes was saturable and reversible (K_d = 1 nM). DTZ417 {(+)-*cis*-3-(acetyloxy)-5-[2-[[2-(3,4-dimethoxyphenyl)ethyl]-dimethylamino]ethyl]2,3-dihydro-2-(4-methyoxyphenyl)-1,5-benzothiazepine-4(5*H*)-one}, a quaternary ammonium derivative of DTZ323, inhibited the specific binding of [^{3}H]DTZ323 in a competitive manner with a K_i value of 41 ± 1 nM, which was very close to the K_i value of diltiazem (159 ± 9 nM) at 25° (17). Thus, the affinity of DTZ417 for the BTZ binding site is sufficiently high to be useful for localizing the BTZ binding site.

The project was supported by a Grant-in-Aid from the Ministry of Education, Science, Sports and Culture, Japan.

ABBREVIATIONS: DHP, 1,4-dihydropyridine; PAA, phenylalkylamine; BTZ, 1,5-benzothiazepine; $I_{Ca(L)}$, Ca^{2+} current through L-type Ca^{2+} channel; I-V, current-voltage; HP, holding potential; EGTA, ethylene glycol bis(β-aminoethyl ether)-*N*,*N*,*N*′,*N*′-tetraacetic acid; HEPES, 4-(2-hydroxyethyl)-1-piperazineethanesulfonic acid.

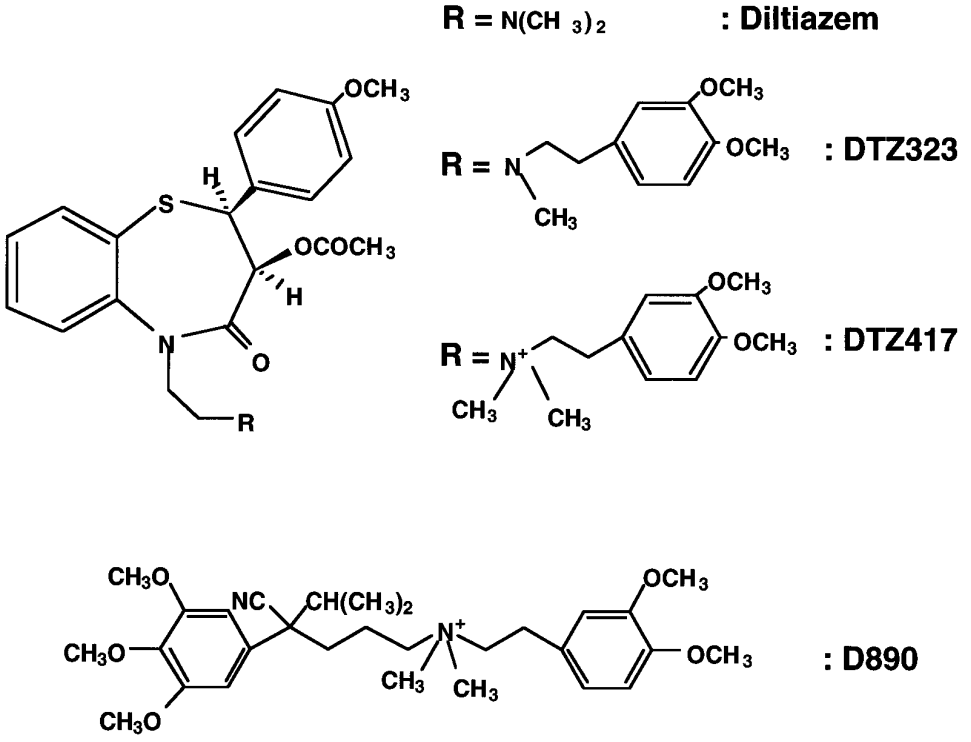

Fig. 1. Chemical structures of Ca^{2+} channel blockers used in this study.

The aim of this study was to determine the side of the transmembrane L-type Ca^{2+} channel protein from which BTZ Ca^{2+} channel blockers gain access to the binding site. We applied DTZ417 from inside or outside of the cardiac myocytes, and we demonstrated that DTZ417 suppresses $I_{Ca(L)}$ preferentially from the outside of the membrane. We conclude that the BTZ binding site localizes on the extracellular side of the α_1 subunit of cardiac L-type Ca^{2+} channel.

Materials and Methods

Cell preparation. Ventricular myocytes were isolated enzymatically from hearts of male Hartley guinea pigs (weight, 200–500 g) according to the method described by Cavalié *et al*. (18) and Adachi-Akahane *et al*. (19). Briefly, the animals were anesthetized, and the ascending aorta was cannulated *in situ*. The heart was perfused at 37° by the Langendorff method, first with nominally Ca^{2+}-free Tyrode's solution and then with collagenase solution. Subsequently, the enzyme solution was washed out with KB solution (20) (containing 70 mM potassium glutamate, 25 mM KCl, 10 mM oxalic acid, 10 mM KH_2PO_4, 10 mM taurine, 11 mM glucose, 10 mM HEPES, 0.5 mM EGTA, pH 7.4, adjusted with KOH). The ventricle was cut into small pieces and dissociated by gentle stirring at 37°. The dissociated cells were kept in the KB solution at 4° and used within 12 hr. The normal Tyrode's solution had the following composition: 135 mM NaCl, 5.4 mM KCl, 1 mM $MgCl_2$, 1.8 mM $CaCl_2$, 11 mM glucose, and 5 mM HEPES-Tris, pH 7.4. Calcium was omitted in the Ca^{2+}-free Tyrode's solution. The collagenase solution was made by adding 70–80 units/ml collagenase (Collagenase-S-1; Nitta Gelatin, Osaka, Japan) and 14.4 μM $CaCl_2$ to the Ca^{2+}-free Tyrode's solution.

Solutions. The internal solution was composed of 80 mM CsCl, 40 mM CsOH, 5 mM MgATP, 10 mM EGTA, and 10 mM HEPES, pH 7.4 adjusted with HCl. For drug applications from the intracellular side, drugs were dissolved in the internal solution.

All experiments were carried out at room temperature (22–25°). The recording chamber (volume, 0.3 ml) was continuously perfused first with Tyrode's solution (120 mM NaCl, 4 mM KCl, 2 mM $CaCl_2$, 2 mM $MgCl_2$, 10 mM glucose, 5 mM HEPES, pH 7.4 adjusted with NaOH). After gigaseal formation and rupture of the membrane patch, the external solution was changed to the Na^+/K^+-free solution containing 120 mM tetraethylammonium chloride, 4 mM CsOH, 2 mM $CaCl_2$, 2 mM $MgCl_2$, 10 mM glucose, and 5 mM HEPES, pH 7.4 adjusted with HCl.

Patch-clamp recording. Currents were recorded using the whole-cell configuration of the patch-clamp technique (21). The cells were placed in a chamber (volume, 0.3 ml) attached to the stage of an inverted microscope (IMT-2; Olympus, Tokyo, Japan). The tip resistances of the fire-polished microelectrodes (borosilicate glass) were 1.5–3.3 MΩ when filled with the internal solution. Series resistance was within three times the tip resistance of the patch electrodes. Recordings were carried out using an Axopatch 1C amplifier (Axon Instruments, Burlingame, CA) with a 100-MΩ headstage, low-pass filtered at 1 or 2 kHz, and digitized at 10 kHz. The pCLAMP software (version 5.5, Axon Instruments) was used to generate voltage-clamp protocols and acquire data.

For internal application, the diffusion half-time of DTZ417 was estimated to be 24 min according to the methods of Pusch and Neher (22) with the average membrane capacitance of the cells (80 pF) and a molecular mass of DTZ417 (M_r 578.71).

Data analysis. All data were digitized online, stored on a computer hard disk, and analyzed using the pCLAMP software. Peak detection was performed with Clampan software, and the rate of inactivation of $I_{Ca(L)}$ was calculated with Clampfit programs. When $I_{Ca(L)}$ was measured, leak subtraction was performed either by subtracting the current measured in the presence of 0.1 mM $CdCl_2$ or by using the P/-4 protocol. In graphs in which the data points represent the results of multiple experiments, the data points were expressed as mean ± standard error. In some of figures, capacitative currents of traces are truncated when they exceeded 500 pA.

Steady state inactivation curves were fitted using SigmaPlot software (Jandel Scientific, San Rafael, CA). Curve fitting for the dose-response curves was performed, and IC_{50} values were calculated using GraphPAD Prism (GraphPAD Software, San Diego, CA).

Statistical significance was assessed with Student's *t* test for simple comparisons or analysis of variance with Bonferroni's multiple *t*

test for multiple comparisons; differences at $p < 0.05$ were considered to be significant.

Drugs. DTZ417 (M_r 578.71), DTZ323 (M_r 564.71), and diltiazem (M_r 414.5) were kindly supplied by Tanabe Seiyaku (Saitama, Japan). D890 (M_r 499.63) was a gift from Knoll AG (Ludwigshafen, Germany). The structures of these drugs are shown in Fig. 1.

Results

The effects of DTZ417 on $I_{Ca(L)}$ are summarized in Fig. 2. To determine the effects of DTZ417 on the voltage dependence of $I_{Ca(L)}$ (Fig. 2A), I-V relationships were obtained in the absence of DTZ417 and after the blocking action had reached steady state by applying test pulses to +10 mV at 0.067 Hz in the presence of DTZ417 (5 μM). To avoid further accumulation of the use-dependent block by DTZ417, test pulses were applied at a low frequency of 0.033 Hz, which did not allow recovery from the suppression of $I_{Ca(L)}$ by DTZ417 at an HP of −50 mV. DTZ417 markedly suppressed the amplitude of peak $I_{Ca(L)}$ without changing the voltage dependence of the I-V relationships.

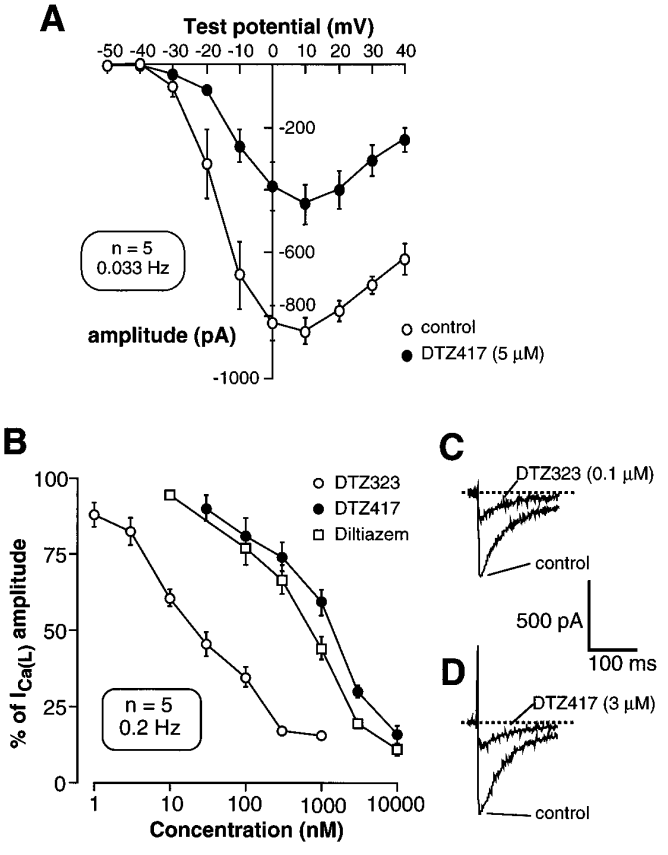

Fig. 2. Effects of DTZ417 on $I_{Ca(L)}$. A, Effect of DTZ417 (5 μM) on I-V relationships (○) before and (●) after application of the drug. $I_{Ca(L)}$ was elicited by depolarizing pulses for 200 msec (0.033 Hz) from an HP of −50 mV. The amplitudes of $I_{Ca(L)}$ were measured after the inhibition of $I_{Ca(L)}$ had reached steady state by giving test pulses (0.067 Hz) to +10 mV in the presence of 5 μM DTZ417. Control $I_{Ca(L)}$ amplitudes at −10, +10, and +30 mV were −670.9 ± 107.9, −849.6 ± 40.2, and −704.1 ± 27.8 pA (five cells), respectively, and those in the presence of DTZ417 at 5 mM were −260.7 ± 53.7, −446.3 ± 64.0, and −309.6 ± 49.6 pA (five cells), respectively. *Curves*, mean ± standard error of five cells. B, Concentration-dependent inhibition of $I_{Ca(L)}$ by the extracellular application of (○) DTZ323 or (●) DTZ417 on the amplitude of $I_{Ca(L)}$. The amplitudes of $I_{Ca(L)}$ evoked by test pulses in the absence of drugs are represented as 100%. $I_{Ca(L)}$ was elicited by depolarizing pulses for 200 msec (0.2 Hz) to +10 mV from an HP of −50 mV. *Points*, mean ± standard error of five cells. C and D, Current traces recorded before and after application of the drugs are superimposed after subtraction of leak currents.

Fig. 2B shows the concentration-response curve for DTZ417 that was obtained after $I_{Ca(L)}$ had reached its steady state level in the presence of given concentrations of DTZ417. The resulting IC_{50} value was 1.2 ± 0.02 μM (30 cells), which was very close to the IC_{50} value of diltiazem (0.63 ± 0.01 μM). The tertiary ammonium derivative DTZ323 also suppressed $I_{Ca(L)}$ with an IC_{50} value of 26 ± 0.08 nM under the same condition. Neither DTZ323 nor DTZ417 changed the rate of the inactivation of $I_{Ca(L)}$ significantly under this condition (Fig. 2, C and D).

The interaction between a Ca^{2+} channel blocker and L-type Ca^{2+} channels is modulated by the state of the channel or by the transmembrane potential, thus showing voltage dependence, use dependence, or both. The effects of DTZ417 (50 μM) on the voltage dependence of the availability of L-type Ca^{2+} channels are shown in Fig. 3. The extent of the inactivation of $I_{Ca(L)}$ was determined by a double-pulse protocol at a frequency of 0.033 Hz. At −90 mV, application of DTZ417 for 3 min produced little tonic block, suggesting that DTZ417 hardly binds to the resting state of the channel. Curves in Fig. 3 were fitted to Boltzmann's distribution:

$$I/I_{max} = \{1 + \exp[(V - V_{0.5})/k]\}^{-1}$$

where $V_{0.5}$ is the midpotential and k is the slope of the curve. The mean control values for $V_{0.5}$ and k in four cells were −18.4 ± 2.3 mV and 3.6 ± 0.5, respectively. Application of DTZ417 shifted the $V_{0.5}$ value to −29.2 ± 3.3 mV (Student's t test, $p < 0.01$) without changing the slope factor (4.5 ± 1.7).

The use-dependent block by extracellularly applied DTZ417 (50 μM) was investigated (Fig. 4). At an HP of −50 mV, the amplitude of $I_{Ca(L)}$ decreased rapidly during successive stimulation in a use-dependent manner. At the more negative HP of −90 mV, less accumulation of block of $I_{Ca(L)}$ was observed. The degree of the use-dependent block, therefore, depended on the HP, as is the case with other Ca^{2+}

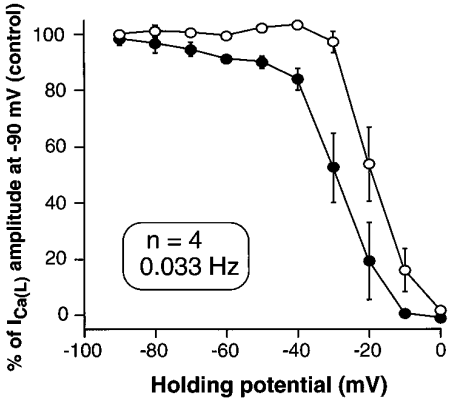

Fig. 3. Effect of DTZ417 (50 μM) on the voltage dependence of $I_{Ca(L)}$ availability. Steady state inactivation curves were obtained (○) before and (●) after exposure to 50 μM DTZ417. Measurement of steady state inactivation was carried out by applying prepossess to produce voltages ranging from −90 to 0 mV for 20 sec from an HP of −90 mV, followed by a test pulse to +10 mV for 200 msec. The peak amplitude of test pulse current was then plotted against the prepulse voltage. The individual peak currents were normalized to the peak $I_{Ca(L)}$ amplitude obtained in the absence of DTZ417 at −90 mV. *Plots*, mean ± standard error of four cells.

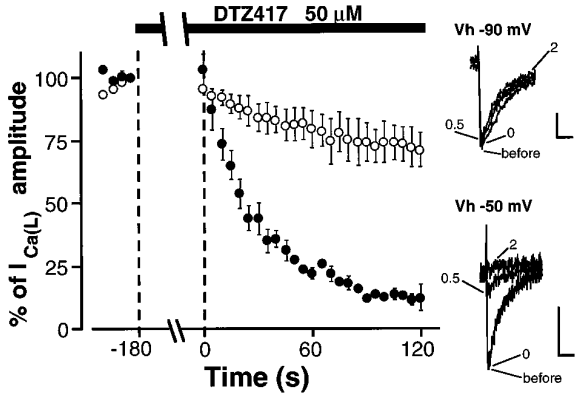

Fig. 4. Voltage dependence of the use-dependent block produced by 50 μM DTZ417. After the peak amplitude of $I_{Ca(L)}$ had reached steady state, cells were exposed to DTZ417 for 3 min without stimulation; then, test pulses were applied in the presence of DTZ417. Data were normalized to $I_{Ca(L)}$ just before the drug application. $I_{Ca(L)}$ were elicited by test pulses (0.2 Hz) to +10 mV from HPs of (●) −50 and (●) −90 mV. Raw current traces recorded at HPs of −90 and −50 mV (*before*) just before application of the drug, (*0*) at the start of the test period, and at (*0.5*) 0.5 and (*2*) 2 min of the test period were superimposed. *Vertical bars*, 200 pA (HP of −90 mV) and 400 pA (HP of −50 mV), respectively; *horizontal bars*, 50 msec.

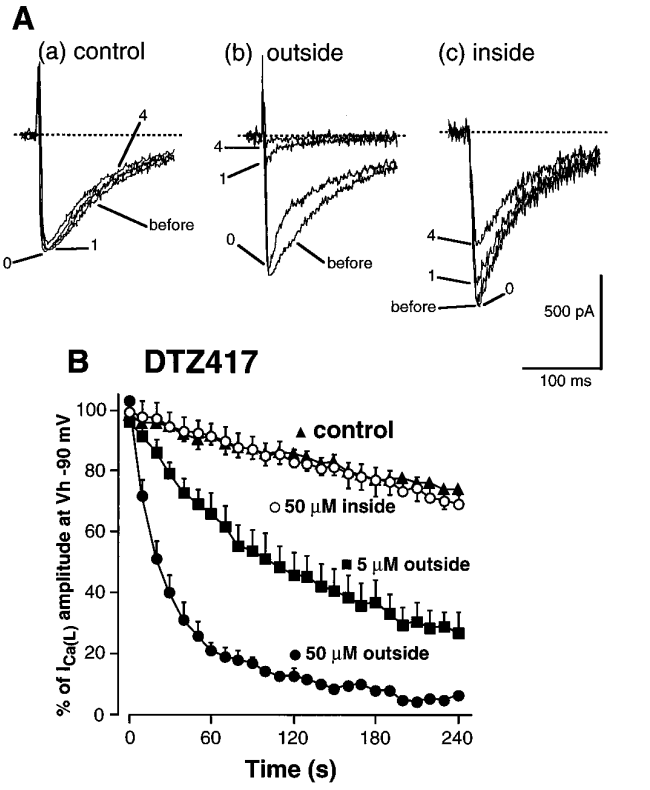

Fig. 5. Effects of the extracellular and intracellular applications of DTZ417. $I_{Ca(L)}$ was elicited by applying test pulses (0.2 Hz) to 10 mV from an HP of −90 mV. The blocking effect was assessed by applying test pulses (0.2 Hz) to 10 mV from an HP of −50 mV for 4 min. $I_{Ca(L)}$ amplitudes during the test period (4 min) at an HP of −50 mV were normalized with $I_{Ca(L)}$ amplitudes at an HP of −90 mV just before changing HP ($I_{ca(L)90}$) as 100%. A, Effects of DTZ417 on $I_{Ca(L)}$: (a) control, (b) extracellularly applied 50 μM DTZ417, and (c) intracellularly applied 50 μM DTZ417. Typical current traces recorded at an HP of −90 mV (*before*) just before changing HP, (*0*) at the start of the test period, and at (*1*) 1 and (*4*) 4 min of the test period at −50 mV were superimposed (a) without subtraction and (b) and (c) after subtraction of leak currents. *Dotted lines*, base-line of the traces. B, Concentration-dependent effects of DTZ417 applied from the extracellular side (5 μM, ■, eight cells; 50 μM, ●, seven cells) in comparison with the intracellular application (50 μM, ○, eight cells). *Control* (▲, eight cells), data in the absence of drugs.

channel blockers (4). The peak amplitudes and the rates of inactivation of the first $I_{Ca(L)}$ in the presence of DTZ417 were the same as those of control at −90 and −50 mV, suggesting that no tonic block took place at either potential.

To compare the onset of the effects of drugs on $I_{Ca(L)}$ produced by extracellular and intracellular applications of drugs (Fig. 5–7). we took advantage of the voltage dependence and the exclusive use dependence of DTZ417 and DTZ323. Thus, we used the voltage protocol (Fig. 4) described by Kass *et al.* (13) and Adachi-Akahane *et al.* (19) with a small modification as follows: First, the cell was maintained at an HP of −90 mV. $I_{Ca(L)}$ was elicited by depolarizing pulses (200 msec) to +10 mV at 0.067 Hz for 4–6 min until $I_{Ca(L)}$ became stable. Then, the frequency was increased to 0.2 Hz, and the cell was stimulated for 2 min until $I_{Ca(L)}$ became stable. The external solution with or without the drug was perfused for an additional 4 min with continuous application of test pulses. Then, the test pulse was stopped, and the HP was changed to −50 mV. After 10 sec, test pulses at 0.2 Hz were started again, and changes in the peak $I_{Ca(L)}$ amplitudes were measured for 4 min (test period). For intracellular drug application, drugs were dissolved in the pipette solution, and the same protocol was carried out. We estimated the diffusion rate of the intracellularly applied drugs according to the method of Pusch and Neher (22). The intracellular concentration of DTZ417 at 12–20 min after the membrane rupture was calculated to be 29–44% of the concentration given in patch pipettes. Data were obtained only from the cells in which the run-down of the peak $I_{Ca(L)}$ amplitudes measured at HP −90 mV during 2 min just before the test period was <10%.

Fig. 5, A and B, shows the effects on $I_{Ca(L)}$ of DTZ417 applied from the extracellular and the intracellular sides. Under control conditions in the absence of drugs, the peak amplitudes of $I_{Ca(L)}$ decayed gradually during 4 min of the test period to 77.3 ± 6.5% (eight cells) of the basal $I_{Ca(L)}$ recorded at −90 mV just before change in the HP ($I_{Ca(L)90}$, −533.1 ± 40.2 pA). The extracellularly applied DTZ417 suppressed $I_{Ca(L)}$ in a concentration- and use-dependent manner by changing the HP from −90 to −50 mV. The extracellularly applied DTZ417 at 5 and 50 μM suppressed $I_{Ca(L)}$ to 30.0 ± 5.3% of the basal $I_{Ca(L)90}$ ($p < 0.05$ versus control, eight cells) and 5.2 ± 2.6% ($p < 0.05$ versus control, seven cells), respectively. The intracellular application of DTZ417 at 50 μM did not affect $I_{Ca(L)}$ (69.0 ± 6.6% of $I_{Ca(L)90}$ at the end of the test period; eight cells) or change the rate of inactivation of $I_{Ca(L)}$. The intracellular application of DTZ417 at 0.5 mM suppressed $I_{Ca(L)}$ to 20.8 ± 4.3% (eight cells). However, even $I_{Ca(L)90}$ tended to be smaller than control ($I_{Ca(L)90}$: control, −533.1 ± 40.4 pA, eight cells; 0.5 mM DTZ417, −403 ± 69.3 pA, eight cells) in the presence of such a high concentration (≥0.5 mM) of the intracellular DTZ417.

Fig. 6 shows the effects of D890 applied from inside or outside of the myocytes. The extracellular application of D890 at 0.1 mM did not decrease $I_{Ca(L)}$ (83.0 ± 3.5% at the end of the test period: $I_{Ca(L)90}$, −611.5 ± 24.8 pA, five cells), whereas the intracellular application of the same concentration (0.1 mM) of D890 decreased $I_{Ca(L)}$ in a use-dependent manner without tonic block (47.9 ± 6.3%, $p <$ 0.05 versus

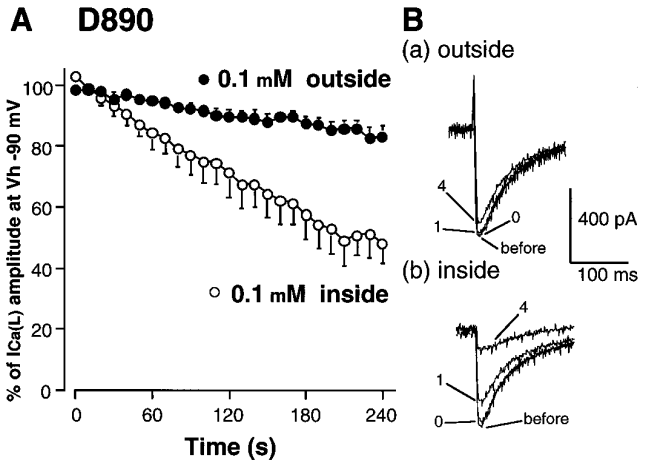

Fig. 6. Effects on $I_{Ca(L)}$ of the extracellular and the intracellular applications of D890. Experimental procedure was described in legend to Fig. 5. A, Comparison of the effects of 0.1 mM D890 between extracellular (●, five cells) and intracellular (○, five cells) application. B, Typical raw current traces recorded in the presence of D890 in the (a) outside and (b) inside at an HP of −90 mV (*before*) just before changing HP, (*0*) at the start of the test period, and at (*1*) 1 and (*4*) 4 min of the test period at −50 mV were superimposed without subtraction.

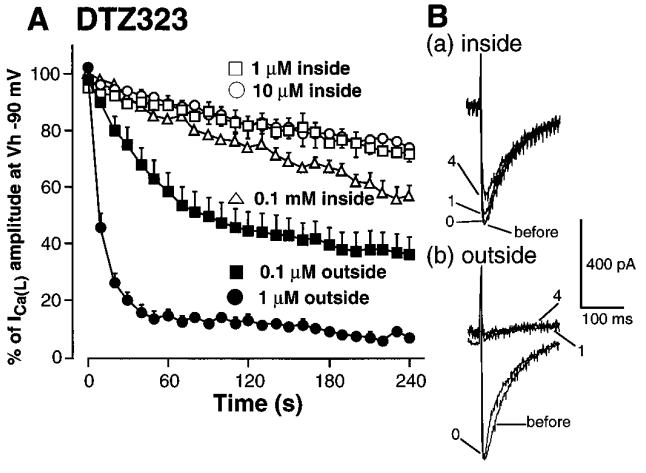

Fig. 7. Effects on $I_{Ca(L)}$ of the extracellular and the intracellular application of DTZ323. Experimental procedure was described in legend to Fig. 5. A, Concentration-dependent effects of DTZ323 applied from the extracellular side (0.1 μM, ■, eight cells; 1 μM ●, eight cells) in comparison with the intracellular application (1 μM, □, eight cells; 10 μM, ○, eight cells, △, three cells). B, Typical raw current traces recorded in the presence of DTZ323 applied from the intracellular side (10 μM, (a) and the extracellular side (1 μM, (b) at an HP of −90 mV (*before*) just before changing HP, (*0*) at the start of the test period, and at (*1*) 1 and (*4*) 4 min of the test period at −50 mV were superimposed without subtraction.

control, five cells). The intracellularly applied D890 (0.1 mM) did not accelerate the decay rate of the first $I_{Ca(L)}$ measured at the beginning of the test period (Fig. 6B, *b*) and did not change the amplitude of $I_{Ca(L)90}$ (−596.7 ± 44.6 pA). The intracellular concentration of D890 at 12–20 min after the membrane rupture was calculated to be 30–45% of the concentration given in patch pipettes. We confirmed that D890 acts only from the inside of the cardiac membrane, as Hescheler *et al*. reported (11). These results exclude the possibility that DTZ417 did not act from the inside because of its poor diffusion from the pipette.

Fig. 7 shows the effects on $I_{Ca(L)}$ of DTZ323 applied from the inside or outside of the membrane. DTZ323 applied from the extracellular side suppressed $I_{Ca(L)}$ in a concentration- and use-dependent manner when the HP was changed from −90 to −50 mV. The extracellularly applied DTZ323 at 0.1 and 1 μM suppressed $I_{Ca(L)}$ to 35.0 ± 5.7% ($p < 0.01$ versus control, eight cells) and 9.0 ± 1.9% ($p < 0.01$ versus control, eight cells), respectively. Again, the intracellular applications of DTZ323 at 1 and 10 μM were almost ineffective on $I_{Ca(L)}$. The $I_{Ca(L)}$ amplitudes recorded at the end of test period were 71.7 ± 2.5% of $I_{Ca(L)90}$ with 1 μM DTZ323 (eight cells) and 75.7 ± 4.3% with 10 μM DTZ323 (eight cells), respectively (amplitude of $I_{Ca(L)90}$: 1 μM DTZ323, −503.1 ± 31 pA, eight cells; 10 μM DTZ323, −606.6 ± 47.5 pA, eight cells). The intracellular application of DTZ323 at 0.1 mM suppressed $I_{Ca(L)}$ to 56.9 ± 3.7% (three cells) without affecting $I_{Ca(L)90}$. These results indicate that DTZ323 suppressed $I_{Ca(L)}$ preferentially from the outside of the membrane, which is consistent with the results obtained with DTZ417.

In Fig. 5A (*b*), in the presence of the extracellularly applied DTZ417 (50 μM), the rate of inactivation of the first $I_{Ca(L)}$ recorded at an HP of −50 mV was significantly faster than that of $I_{Ca(L)90}$ (τ = 38.5 ± 7.7 versus 54.7 ± 8.3 msec, $p < 0.05$, six cells). Similarly, in Fig. 7B (*b*), in the presence of the extracellularly applied DTZ323 at 1 μM, the decay rate of the first $I_{Ca(L)}$ at −50 mV was significantly faster than that of $I_{Ca(L)90}$ (τ = 70.5 ± 6.8 msec at −90 mV versus 60.4 ± 7.3 msec at −50 mV, $p < 0.05$, seven cells). The reason for the change of the inactivation rate of $I_{Ca(L)}$ is not clear. It might be due to the overlapping inward Na^+/Ca^{2+} exchange current activated by Ca^{2+} release from the sarcoplasmic reticulum (23) or to the restitution of I_{Ca} from the use-dependent facilitation (24). Nevertheless, it is unlikely to be due to an open-channel-blocking effect of DTZ417, which did not change the rate of inactivation of $I_{Ca(L)}$ when the use-dependent effect of DTZ417 was assessed at either −50 or −90 mV (Fig. 4).

Discussion

The BTZ binding domain has been assumed to be located near the DHP and PAA binding domains because of their allosteric interactions found in radioligand studies (1). The quaternary benzazepine, SQ32,428, which inhibited (−)-*cis*-[^{3}H]desmethoxyverapamil and (+)-*cis*-[^{3}H]diltiazem binding in a competitive manner, seems to be effective only from the outside of the cell membrane (25, 26). It has been reported that the dog coronary vasodilating activities of BTZs were selective for D-*cis* isomer (27). Radioligand binding experiments also showed that the binding of diltiazem to the BTZ binding site is highly stereospecific for D-*cis* isomer (28). Thus, D-*cis* isomer of BTZ structure seems to be critical for the pharmacological effect of BTZs. DTZ417, as well as DTZ323, is a D-*cis* isomer of the BTZ derivatives that conserve the BTZ structures. Therefore, we used DTZ417 and DTZ323 in the current study.

To determine the sidedness of the functional binding site of BTZ Ca^{2+} channel blocker, we used the permanently charged quaternary derivative DTZ417, which is considered to be impermeable through cell membranes. We showed that DTZ417, like DTZ323, suppresses $I_{Ca(L)}$ in a voltage- and use-dependent manner without tonic block from the outside (Figs. 2 and 3). However, the quaternarization reduced the affinity of DTZ417, as is often the case with quaternary

diltiazem (19) and other Ca^{2+} channel blockers (29). In guinea pig ventricular myocytes, the IC_{50} value of DTZ417 for inhibition of $I_{Ca(L)}$ was 44 times higher than that of DTZ323 when measured at an HP of −50 mV (Fig. 2B). In rabbit crude T tubule membrane, DTZ417 inhibited the specific binding of [^{3}H]DTZ323 in a competitive manner. The K_i value for DTZ417 was 13 times that for DTZ323 (16). In both cases, DTZ417 exhibited the highest affinity for L-type Ca^{2+} channels of all BTZ quaternary derivatives studied to date.

We applied DTZ417 from the extracellular and intracellular sides of the native cardiac cell membrane. We elevated the HP from −90 to −50 mV at >11 min after membrane rupture, which should allow >29% of the pipette concentration of DTZ417 to diffuse into myocytes (22). DTZ417 (50 μM) had no effect from the inside, whereas even at 5 μM, extracellularly applied DTZ417 inhibited $I_{Ca(L)}$ in a voltage- and use-dependent manner. However, a high concentration of DTZ417 (0.5 mM) was effective from both sides of the membrane, suggesting distinct low affinity binding sites to which DTZ417 approaches from the intracellular side.

Adachi-Akahane *et al*. (19) reported that the quaternary derivative of diltiazem was equally effective from both the extracellular and intracellular sides in guinea pig ventricular myocytes. Because the affinity of quaternary diltiazem for the L-type Ca^{2+} channels is ~40 times lower than that of diltiazem, it required quite a high concentration (0.1–1 mM) for suppression of $I_{Ca(L)}$, even at the HP of −40 mV. Such a high concentration of quaternary diltiazem could cause the secondary effect, which might be the reason for the complex result. Diltiazem was also effective from both sides of the membrane. However, the equipotent concentration for the intracellular application was 1000 times higher than that for the extracellular application (30), suggesting that diltiazem preferentially approaches its binding site from the outside of the membrane.

Both DHP and BTZ binding sites are accessible from the extracellular side of the membrane. However, these Ca^{2+} channel blockers seem to interact with the channel protein at different sites. Because charged DHP confer different modulatory characteristics, such as tonic blocking action (31), on L-type Ca^{2+} channel function compared with the charged BTZ studied in the current investigation, this observation suggests that the charged drugs are acting at different sites.

The BTZ binding site has been proposed, based on the photoaffinity labeling and immunoprecipitation experiments, to be the S5-6 linker region of domain IV and/or S6 segment of domain III (14, 15). Thus, the binding site may be localized in the channel pore or the transmembrane region. It may be the reason why DTZ323, DTZ417, and diltiazem (BTZs) have little tonic blocking effect from the extracellular side on the resting state of the channel. At potentials more depolarized than −30 mV (Fig. 3), the change of the conformation around the pore-forming region may allow BTZs to gain access to the binding site from the outside of the membrane.

We conclude from our results that the high affinity binding domain of BTZ Ca^{2+} channel blocker is located on the extracellular domain of the cardiac L-type Ca^{2+} channel protein. The identification of the critical binding site for Ca^{2+} channel blockers for suppression of $I_{Ca(L)}$ would be important for understanding the channel gating mechanism and pharmacology of Ca^{2+} channel blockers.

Acknowledgments

We thank Tanabe Seiyaku for the generous supply of DTZ417, DTZ323, and diltiazem and Knoll AG for the gift of D890.

References

1. Glossmann, H., D. Ferry, A. Goll, J. Striessnig, and G. Zernig. Calcium channels and calcium channel drugs: recent biochemical and biophysical findings. *Arzneim. Forsch.* **35:**1917–1935 (1985).
2. Catterall, W. A., and J. Striessnig. Receptor sites for Ca^{2+} channel antagonists. *Trends Pharmacol. Sci.* **13:**256–262 (1992).
3. Spedding, M., and R. Paoletti. III. Classification of calcium channel and the sites of action of drugs modifying channel function. *Pharmacol. Rev.* **44:**363–376 (1992).
4. McDonald, T. F., S. Pelzer, W. Trautwein, and D. Pelzer. Regulation and modulation of calcium channels in cardiac, skeletal, and smooth muscle cells. *Physiol. Rev.* **74:**365–506 (1994).
5. Nakayama, H., M. Taki, J. Striessnig, H. Glossmann, W. A. Catterall, and Y. Kanaoka. Identification of 1,4-dihydropyridine binding regions within the α1 subunit of skeletal muscle Ca^{2+} channels by photoaffinity labeling with diazepine. *Proc. Natl. Acad. Sci. USA* **88:**9203–9207 (1991).
6. Striessnig, J., B. J. Murphy, and W. A. Catterall. Dihydropyridine receptor of L-type Ca^{2+} channels: identification of binding domains for [^{3}H](+)-PN200–110 and [^{3}H]azidopine within the α_1 subunit. *Proc. Natl. Acad. Sci. USA* **88:**10769–10773 (1991).
7. Striessnig, J., H. Glossmann, and W. A. Catterall. Identification of a phenylalkylamine binding region within the α_1 subunit of skeletal muscle Ca^{2+} channels. *Proc. Natl. Acad. Sci. USA* **87:**9108–9112 (1990).
8. Kalasz, H., T. Watanabe, H. Yabana, K. Itagaki, K. Naito, H. Nakayama, A. Schwartz, and P. L. Vaghy. Identification of 1,4-dihydropyridine binding domains within the primary structure of the α_1 subunit of the skeletal muscle L-type calcium channel. *FEBS Lett.* **331:**177–181 (1993).
9. Tang, S., A. Yatani, Y. Bahinski, Y. Mori, and A. Schwartz. Molecular localization of regions in the L-type calcium channel for dihydropyridine action. *Neuron* **11:**1–20 (1993).
10. Granner, M., Z. Wang, S. Hering, J. Striessnig, and H. Glossmann. Transfer of 1,4-dihydropyridine sensitivity from L-type to class A (BI) calcium channels. *Neuron* **16:**207–218 (1996).
11. Hescheler, J., D. Pelzer, G. Trube, and W. Trautwein. Does the organic calcium channel blocker D600 act from inside or outside on the cardiac cell membrane? *Pflueg. Arch. Eur. J. Physiol.* **393:**287–291 (1982).
12. Affolter, H., and R. Coronado. Sidedness of reconstituted calcium channels from muscle transverse tubules as determined by D600 and D890 blockade. *Biophys. J.* **49:**767–771 (1986).
13. Kass, R. S., J. P. Arena, and S. Chin. Block of L-type calcium channels by charged dihydropyridines. *J. Gen. Physiol.* **98:**63–75 (1991).
14. Watanabe, T., H. Kalasz, H. Yabana, A. Kuniyasu, J. Mershon, K. Itagaki, P. L. Vaghy, K. Naito, H. Nakayama, and A. Schwartz. Azidobutyryl clentiazem, a new photoactivatable diltiazem analog, labels benzothiazepine binding sites in the α_1 subunit of the skeletal muscle calcium channel. *FEBS Lett.* **334:**261–264 (1993).
15. Kraus, R., B. Reichl, S. D. Kimball, M. Grabner, B. J. Murphy, W. A. Catterall, and J. Striessnig. Identification of benz(othi)azepine-binding regions within L-type calcium channel α1 subunits. *J. Biol. Chem.* **271:** 20113–20118 (1996).
16. Nagao, T., M. Hagiwara, J. Kurokawa, and S. Adachi-Akahane. High affinity binding of DTZ323, a novel 1,5-benzothiazepine derivative, to diltiazem binding site. *Can. J. Physiol. Pharmacol.* **72:** suppl. I, 522 (1994).
17. Kurokawa, J., S. Adachi-Akahane, and T. Nagao. Quaternary 1,5-benzothiazepine derivative (DTZ417) acts only from extracellular side of the membrane in ventricular myocytes. *Heart Vessels* **(Suppl. 10)** 21 (1995):
18. Cavalié, A., R. Ochi, D. Pelzer, and W. Trautwein. Elementary currents through Ca^{2+} channels in guinea pig myocytes. *Pflueg. Arch. Eur. J. Physiol.* **398:**284–297 (1983).
19. Adachi-Akahane, S., Y. Amano, R. Okuyama, and T. Nagao. Quaternary diltiazem can act from both sides of the membrane in ventricular myocytes. *Jpn. J. Pharmacol.* **61:**263–266 (1993).
20. Isenberg, G., and U. Klockner. Calcium tolerant ventricular myocytes prepared by preincubation in a "KB medium." *Pflueg. Arch. Eur. J. Physiol* **395:**6–18 (1982).
21. Hamill, O. P., A. Marty, E. Neher, B. Sakmann, and F. J. Sigworth. Improved patch-clamp techniques for high-resolution current recording from cells and cell-free membrane patches. *Pflueg. Arch. Eur. J. Physiol.* **391:**85–100 (1981).
22. Pusch, M, and E. Neher. Rates of diffusional exchange between small cells and a measuring patch pipette. *Pflueg. Arch. Eur. J. Physiol.* **411:**204–211 (1988).
23. Spido, K. R., G. Callewaert, and E. Carmeliet. Inhibition and rapid recovery of Ca^{2+} release from sarcoplasmic reticulum in guinea pig ventricular myocytes. *Circ. Res.* **76:**102–109 (1995).
24. Zygmunt, A. C., and J. Mayliet. Stimulation-dependent facilitation of the high threshold calcium current in guinea-pig ventricular myocytes. *J. Physiol.* **428:**653–671 (1990).

25. Hering, S., A. Savchenko, C. Strübing, M. Lakitsch, and J. Striessnig. Extracellular localization of the benzothiazepine binding domain of L-type Ca^{2+} channels. *Mol. Pharmacol.* **43:**820–826 (1993).
26. Seydl, K., D. Kimball, H. Schindler, and C. Romanin. The benzazepine/benzothiazepine binding domain of the cardiac L-type Ca^{2+} channel is accessible only from the extracellular side. *Pflueg. Arch. Eur. J. Physiol.* **424:**552–554 (1993).
27. Nagao, T., H. Narita, M. Sato, H. Nakajima, and A. Kiyomoto. Development of diltiazem, a calcium antagonist: coronary vasodilating and antihypertensive actions. *Clin. Exp. Hypertens. Part A Theory Pract.* **A4:**285–296 (1982).
28. Ikeda, S., J. Oka, and T. Nagao. Effects of four diltiazem stereoisomers on binding d-cis-[^{3}H]diltiazem and (+)-[^{3}H]PN 200–110 to rabbit T-tubule calcium channels. *Eur. J. Pharmacol.* **208:**199–205 (1991).
29. Kwan, Y. W., R. Bangalore, M. Lakitsch, H. Glossmann, and R. S. Kass. Inhibition of cardiac L-type calcium channels by quaternary amlodipine: implications for pharmacokinetics and access to dihydropyridine binding site. *J. Mol. Cell Cardiol.* **27:**253–262 (1995).
30. Adachi-Akahane, S., and T. Nagao. Binding site for diltiazem is on the extracellular side of the L-type Ca^{2+} channel (Abstract). *Circulation* **88** (Suppl. I)**:**I-230 (1993).
31. Bangalore, R., N. Baindur, A. Rutledge, D. J. Triggle, and R. S. Kass. L-type calcium channels: asymmetrical intramembrane binding domain revealed by variable length, permanently charged 1,4-dihydropyridines. *Mol. Pharmacol.* **46:**660–666 (1994).

Send reprint requests to: Taku Nagao, Ph.D., Department of Toxicology and Pharmacology, Faculty of Pharmaceutical Sciences, University of Tokyo, 7–3-1 Hongo, Bunkyo-ku, Tokyo 113, Japan. E-mail:tnagao@mol.f.u-tokyo.ac.jp